Journal of Trace Elements in Medicine and Biology 51 (2019) 226–234

Contents lists available at ScienceDirect

Journal of Trace Elements in Medicine and Biology

journal homepage: www.elsevier.com/locate/jtemb

# Zinc overload mediated by zinc oxide nanoparticles as innovative anti-tumor agent

Nadine Wiesmann[a], Martin Kluenker[b], Philipp Demuth[a], Walburgis Brenner[c], Wolfgang Tremel[b], Juergen Brieger[a,*]

[a] Molecular Tumor Biology, Department of Otorhinolaryngology, Head and Neck Surgery, University Medical Centre of the Johannes Gutenberg University, 55131, Mainz, Germany
[b] Institute of Inorganic Chemistry and Analytical Chemistry, Johannes Gutenberg University, 55128, Mainz, Germany
[c] Department of Gynecology, University Medical Centre of the Johannes Gutenberg University, 55131, Mainz, Germany

ARTICLE INFO

*Keywords:*
Zinc oxide
Nanoparticles
Tumor therapy

ABSTRACT

The predicted global cancer burden is expected to surpass 20 million new cancer cases by 2025. Despite recent advancement in tumor therapy, a successful cancer treatment remains challenging. The emerging field of nanotechnology offers great opportunities for diagnosis, imaging, as well as treatment of cancer. Zinc oxide nanoparticles (ZnO NP) were shown to exert selective cytotoxicity against tumor cells via a yet unknown mechanism, most likely involving the generation of reactive oxygen species (ROS). These nanoparticles are a promising therapeutic opportunity as zinc is a nontoxic trace element and its application in medically-related products is considered to be safe.

We could show that ZnO NP can exert cytotoxic effects on several human tumor cell lines. There can be found ZnO NP concentrations which selectively damage tumor cells while human fibroblasts do not sustain lasting damage. Cytotoxicity is attributable to the release of zinc ions from the nanoparticles outside the cells as well as to a direct cell-nanoparticle interaction. This involves uptake of the particles into the tumor cells. With a silica shell the cytotoxicity can be delayed which can help in the future for a safe transport in the blood stream. Cellular damage finally cumulates in apoptotic cell death via zinc overload within 48 h after treatment with ZnO NP.

A therapeutical perspective could be the targeted accumulation of ZnO NP at the tumor side to induce local zinc overload that substantially damages the tumor cells with no or low side effects. We suggest further studies to explore the potential of ZnO NP as an innovative anti-tumor agent.

## 1. Introduction

Over the last decades research on the biomedical application of nanomaterials has advanced with great strides. Reducing the size of particles from bulk material to nanoscale is accompanied by a modification of their chemical, physical and biological properties [1–3]. These special characteristics allow the NP to interact in a unique manner with cellular biomolecules and thus facilitate the transfer of NP into inner cellular structures [4]. All nanostructured materials have a large percentage of atoms at their surface in common, which leads to high surface reactivity. Despite recent advancements in nanomedicine, research is still far away from achieving a profound understanding of the behavior of nanomaterials in the human body [5,6].

Zinc oxide nanoparticles (ZnO NP) are already used in many different products, for example in sunscreens as UV absorber [7], in the rubber industry as additive, in electronics [8] and their antibacterial properties [9] are exploited for antimicrobial applications in food industry and in lotions for wound healing. Additionally, it has been revealed about ten years ago, that they have the potential to selectively kill tumor cells [10], although the exact mechanism of cytotoxicity is still subject to discussions [11]. The potential use of ZnO NP as an anticancer agent has since then been described by several different

*Abbreviations:* Gy, gray; ZnO NP, zinc oxide nanoparticles; ROS, reactive oxygen species; ZnO@$SiO_2$ NP, zinc oxide nanoparticles with silica coating; NP, nanoparticles; AAS, atomic absorption spectroscopy; TEM, transmission electron microscopy; CMA, cellular metabolic activity; SCC, squamous cell carcinoma; RT, room temperature; NSCLC, non-small cell lung cancer; HNSCC, head and neck squamous cell carcinoma; PI, propidium iodide; FCS, fetal calf serum; cLSM, confocal laser scanning microscopy; HU, heat-up

* Corresponding author.
*E-mail address:* brieger@uni-mainz.de (J. Brieger).

https://doi.org/10.1016/j.jtemb.2018.08.002
Received 21 December 2017; Received in revised form 2 August 2018; Accepted 3 August 2018

studies performed with different tumor entities [12–24].

The involvement of reactive oxygen species (ROS) and DNA damage is recognized as verified [25] but it is still debated whether the toxicity of ZnO NP can be attributed to the particles themselves or to dissolved zinc ions and whether particles can enter cancer cells where they could evoke additional damage. In the current study we will shed light on those questions. Additionally, we want to reveal which mode of cell death is induced by ZnO NP and distinguish between apoptosis and necrosis.

Profound understanding of the intracellular processes after ZnO NP exposure will further advance our understanding of the toxicity mechanism of ZnO NP and push forward efforts to make these versatile particles applicable in a biomedical setting as anti-tumor agent.

## 2. Materials and methods

### 2.1. Nanoparticle synthesis

The solvothermal synthesis of the unmodified ZnO NP (15–18 nm) was adapted from Cheng et al. with some modifications [26]. 5 mmol of $Zn(ac)_2{\cdot}2\ H_2O$ was dissolved in 10 mL methanol and gently shaken. 20 mL of tetramethylammonium hydroxide 25% (w/w) in methanol were slowly added and the mixture was stirred for 20 min. The reaction mixture was transferred to a 50 mL teflon-lined stainless-steel autoclave and heated at 50 °C for 24 h. The colourless precipitate was separated by centrifugation and washed twice with deionized water. Finally, the product was dispersed in ethanol and stored at RT for long term storage or dried in air for short term storage.

The APTES-FITC conjugate synthesis for dye functionalization of $ZnO@SiO_2NP$ was carried out by dissolving 0.003 mmol of FITC in 0.5 mL of dry DMSO (solution 1). 0.009 mmol of APTES were dissolved in 0.5 mL of dry DMSO (solution 2). Afterwards, solution 1 was added to solution 2 and the mixture was stirred overnight at RT under exclusion of light. The APTES-FITC conjugate can be stored at 8 °C for up to 2 d.

The synthesis of "heatup" ZnO (HU) NP was adapted from Tahir et al. with some modifications [27]. 0.5 mmol $Zn(ac)_2{\cdot}2\ H_2O$ (pre-annealed at 110 °C for 10 min) were dispersed in 4 mL of benzyl alcohol, 3 mL of oleylamine and 2 mL of 1-octadecene under inert gas conditions and stirred for 5 min. The mixture was heated to 120 °C for 20 min and then heated to 230 °C for 30 min. Afterwards, the mixture was slowly cooled to RT. The colourless product was precipitated and separated by centrifugation, dispersed in cyclohexane and washed twice by adding ethanol (cyclohexane:ethanol = 1:2). Finally, the product was dispersed in cyclohexane and stored at RT.

The synthesis of $ZnO@SiO_2NP$ with HU ZnO NP was carried out using a reverse microemulsion technique. 2 g of Igepal CO-520 and 100 µL of oleylamine were dispersed in 40 mL of cyclohexane. The mixture was ultrasonicated for 15 min. 10 mg of HU ZnO NP were added and the mixture was ultrasonicated for additional 15 min. 150 µL of ammonium hydroxide solution of pH 11.5 were added and the mixture was stirred for additional 10 min. The stirring speed was increased to maximum and 120 µL of TEOS were injected rapidly. After 20 min 5 µL of the preformed APTES-FITC conjugate was added. The mixture was stirred overnight at maximum stirring speed. In the morning and evening of the next day 15 µL of TEOS each were added, and the mixture was again stirred overnight. 100 µL of PEGTES were subsequently added and the mixture was stirred for additional 4 h. The precipitate was separated by centrifugation, dispersed in ethanol and washed twice by adding cyclohexane (ethanol:cyclohexane = 1:2). Finally, the product was dispersed in ethanol and stored at 8 °C. For all experiments the same batch of ZnO NP and $ZnO@SiO_2$ NP was used.

### 2.2. Nanoparticle characterization

The NP were characterized by transmission electron microscopy (*TEM*), *X-ray diffraction*, and *ζ-potential* measurements. Samples for *TEM* were prepared by placing a drop of NP dispersion in cyclohexane on a carbon coated copper grid. TEM images for the characterization of size and morphology were obtained using a FEI Tecnai 12 equipped with $LaB_6$ source at 120 kV and a twin-objective together with a Gatan US1000 CCD-camera (2kx2k pixels). *X-ray diffraction* patterns were recorded on a Bruker AXS D8 Advance diffractometer equipped with a SolX energy dispersive detector in reflection mode using unfiltered MoKα radiation. Crystalline phases were identified according to the PDF–2 database using Bruker AXS EVA 10.0 software. Measurements of the ζ-potential of the NP were performed using a Zetasizer Nano ZS from Malvern Instruments using a disposable capillary cell. Typically, 1 mL aliquots of each sample were injected into the capillary cell and 5-10 measurements per sample were performed at 25 °C.

### 2.3. Cell culture and nanoparticle treatment conditions

For the study we chose tumor cell lines of different origin: A549 (non-small cell lung cancer (NSCLC)), HeLa (cervix carcinoma), HNSCCUM-02 T (tongue, squamous cell carcinoma (SCC)), T24 (urothelial carcinoma), RPMI-2650 (nasal septum, SCC) and FaDu (pharynx, SCC). The head and neck squamous cell carcinoma (HNSCC) cell line HNSCCUM02T was previously established and characterized in our laboratory [28]. The other cell lines were purchased from DSMZ (German Collection of Microorganisms and Cell Cultures, Braunschweig, Germany). Their identity was verified by STR analysis. As representatives of healthy, non-tumorigenic tissue, human fibroblasts isolated from oral mucosa were chosen as primary control cells. They were isolated from material obtained from patients who underwent surgery at the University Medical Center, Mainz, Germany as previously described [29]. Cells were maintained in DMEM/Ham's F12 (Sigma-Aldrich, St. Louis, USA) supplemented with 10% FCS (fetal calf serum; Sigma-Aldrich, St. Louis, USA) and antibiotics (100 U/mL penicillin and 100 mg/mL streptomycin) at 37 °C in 5% $CO_2$.

ZnO NP were stored airtightly sealed at 8 °C and 1 mg/mL ZnO NP dispersions were freshly prepared immediately before each experiment with high-purity water (Ampuwa®, Fresenius Kabi GmbH, Bad Homburg, Germany). To disperse the NP, they were sonicated 5 min with 220–240 V and 37 kHz in an Elmasonic S 40 sonicator (Elma Schmidbauer GmbH, Singen, Germany) and sedimentation was prevented by pipetting up and down. $ZnCl_2$ solution was obtained from Sigma-Aldrich (0.1 M solution, Sigma-Aldrich, St. Louis, Missouri, USA)) and diluted to the proper concentration with high-purity water. Cells were treated with the indicated amount of $ZnCl_2$ or ZnO NP for 4 h, followed by an exchange of the cell culture medium.

### 2.4. Atomic absorption measurements

Atomic absorption spectroscopy (AAS) measurements were conducted using a Perkin Elmer 5100 ZL AA spectrometer with a Zeeman Furnace Module and a Zn hollow cathode lamp at 213.9 nm and air/acetylene mixture. For zinc ion detection the sample was treated with aqua regia overnight to dissolve any ZnO and denature any proteins. Afterwards the sample was diluted with deionized water. Samples were analysed using the whole flame width to ensure maximum ionization and reduced matrix effects. A 3-point calibration was carried out with 9 measurements for each concentration. Between sample measurements the instrument was rinsed with aqua regia and deionized water.

### 2.5. Confocal laser scanning microscopy

To visualize intracellular zinc, we used FluoZin™-3-AM, LysoTracker® Deep Red was used to stain the lysosomes and CellMask™ Orange Plasma membrane stain was used to visualize the cell contours (all dyes from Thermo Fisher Scientific, Waltham, Massachusetts, USA). The dyes were used according to manufacturers' specifications. After

45 min of FluoZin™-3-AM preincubation, medium was replaced by 2 mL buffer (100 mM NaCl, 10 mM Tris, pH 7.4) and intracellular increase of zinc after ZnO NP treatment was measured every minute for 1 h by cLSM. Confocal images were acquired on a Leica TCS SP5 (Leica Microsystems, Wetzlar, Germany).

### 2.6. Viability measurements

For the analysis of the cellular viability after treatment with ZnO NP or ZnO@$SiO_2$, we assessed the cellular metabolic activity (CMA) of the cells with the alamar-Blue® (Biozol Diagnostica, Eching, Germany) reagent. 10.000 cells per well were seeded in a 96 well plate and cultivated overnight for adherence. The next day, cells received fresh cell culture medium and were treated with the indicated amount of NP. Treatment with the equivalent amount of water served as positive control (= untreated) and treatment with 70% ethanol as negative control. To all wells 10% alamar-Blue® was added at the indicated time points and the samples were incubated for additional 3 h at 37 °C. The results were obtained using a plate reader (Fluoroskan Ascent Microplate reader, Thermo Fisher Scientific, Waltham, Massachusetts, US; ex: 540 nm, em: 600 nm) and normalized to control cells ( = 100% viability).

### 2.7. Light microscopy

For light microscopical imaging of cellular morphology after NP treatment, cells were seeded in 25 $cm^2$ cell culture flasks and treated with NP according to the standard procedure. Pictures were taken prior to the treatment and after 2 h, 4 h, 8 h, and 24 h with a fluorescence microscope AxioVert 200 M (Zeiss, Jena, Germany). Cells treated with an equivalent amount of water served as control.

### 2.8. Flow cytometric assessment of apoptosis and necrosis

Apoptosis and necrosis were assessed via staining with propidium iodide (PI) and AnnexinV-FITC and subsequent flow cytometric analysis. In short, A549 cells were treated with the indicated amount of ZnO NP or $ZnCl_2$ for 4 h, then cell culture medium was changed, and cells were harvested 4 h, 12 h, 18 h, 24 h, 48 h, 72 h, and 96 h after the beginning of the treatment. Cells treated with an equivalent amount of water served as control. Afterwards cells were stained with PI (Thermo Fisher Scientific, Waltham, Massachusetts, USA) and AnnexinV-FITC (BioLegend™, San Diego, California, USA) according to manufacturers' specifications. Cell samples were then analysed with a BD FACS Canto II flow cytometer (Becton Dickinson, Francklin Lakes, New Jersey, USA) and data was analysed via the cytobank platform (https://www.cytobank.org/, Cytobank, Inc., Santa Clara, California, USA). Cells without staining, were considered to be alive, cells which were single stained by PI to be necrotic and single stained by AnnexinV-FITC to be apoptotic and those which were stained by PI and AnnexinV-FITC to be dead.

## 3. Results

### 3.1. Particle characterization and zinc ion release

Transmission electron microscopy (TEM) showed that the solvothermally synthesized ZnO NP were of spherical shape. Their size ranged from 5 to 15 nm in diameter (Fig. 1A). The ZnO@$SiO_2$ NP were coated by a silica-shell of about 21 nm thickness. In the TEM images the dark ZnO core could be seen within the light silica-shell (Fig. 1B) due to their different scattering contrast. X-ray diffraction (XRD) patterns of ZnO NP were obtained and all reflection could be assigned to the hexagonal wurtzite-type ZnO structure with the lattice parameters a = 3.24 Å and c = 5.20 Å and space group (SG) P63mc (No. 186) (Fig. 1C). To further characterize the particles, their ζ-potential was determined. In water the ZnO NP revealed a ζ-potential of −67 mV and the ZnO@$SiO_2$ NP a ζ-potential of -2,8 mV up to 0 mV depending on the dye loading.

One important property of all metal oxide NP is their stability against dissolution. Over the course of time the metal ions are set free from the particle and contribute to the cellular reaction to the particle treatment. Thus, we assessed the amount of released zinc ions after 4 h and after 24 h in different media namely water, Tris-NaCl buffer, pure cell culture medium and cell culture medium supplemented with 10% FCS (fetal calf serum) (Fig. 1D). In total 100 µg/mL ZnO NP could theoretically set free 1,23 mM zinc ions but only at most about 250 to 300 µM zinc ions were released. In cell culture media the equilibrium was already established after 4 h and the amount of additional zinc ions that were released within further 20 h was small. On the contrary, the equilibrium in water was not yet established after 4 h and additional zinc ions were liberated until measuring time after 24 h. In total, in cell culture medium with FCS more zinc ions are released than in pure cell culture medium.

### 3.2. Cellular toxicity

To analyze the cytotoxicity of ZnO NP four different cancer cell lines (A549, HeLa, HNSCCUM-02T, T24) were treated with 100 µg/mL ZnO NP for 4 h and their morphology was studied under the light microscope. It could be seen that ZnO NP treatment in all cell lines resulted in a pronounced rounding of the cells which was accompanied by an increase in granularity and finally detachment of the cells from the cell culture plate (Fig. 2A). Four hours after the beginning of the treatment, when the cell culture medium was changed, and excessive particles were washes away – cells were still attached to the cell culture plate (second row). Within the next four hours cells began to detach from the cell culture plate and nearly all cells showed a rounded shape (third row). 24 h after beginning of the treatment most cells were detached from the plate and exhibited a granular morphology (last row).

This observation could also be verified by flow cytometry, where a shift of the cell population to higher SSC (side-scatter) and lower FSC (forward-scatter) values could be seen (representative picture in Fig. 2B). This indicates a decrease in cell size and an increase in granularity.

To evaluate the cellular toxicity of ZnO NP to tumor cells on the one hand and healthy tissue on the other hand we compared A549 tumor cells, and fibroblasts of healthy donors (Fig. 3). The cellular viability of the different cell types after treatment with 100 µg/mL, 50 µg/mL or 10 µg/mL ZnO NP was assessed with an alamarBlue® assay after 4 h, 8 h, 12 h and 24 h. The assay measures the cellular metabolic activity (CMA), the absorbance readings of the untreated cells (positive control) were set to 100% and all test samples were normalized to this value. Treatment of cells with 100 µg/mL ZnO NP reduced cellular viability within 4 h below 25% of the untreated control cells for A549 tumor cells as well as for fibroblasts. A549 cells and fibroblasts were able to slightly recover from the treatment after 8 h but viability was further reduced after 12 h and 24 h. For the intermediate dosage of 50 µg/mL ZnO NP we saw a reduction of tumor cell viability to 70% within 12 h compared to untreated control cells while fibroblasts remained largely unaffected by that dosage. A549 cells and fibroblasts were able to cope with 10 µg/mL ZnO NP without sustaining lasting damage.

Next, we tested whether the cellular toxicity of ZnO NP could be traced back to the particles themselves or whether it is attributable to released zinc ions that are set free extracellularly within 4 h of incubation with the NP. To quantify the effect attributed to the released zinc ions, a 100 µg/mL ZnO NP dispersion was incubated for 4 h under cell culture conditions and thereupon remaining particles were separated by centrifugation. Then cells were either incubated directly with ZnO NP for 4 h or with the supernatant of the particles (Fig. 4). Both treatments resulted in a reduction of cellular viability of tumor cells within 4 h. Then cells were washed and incubated with fresh cell

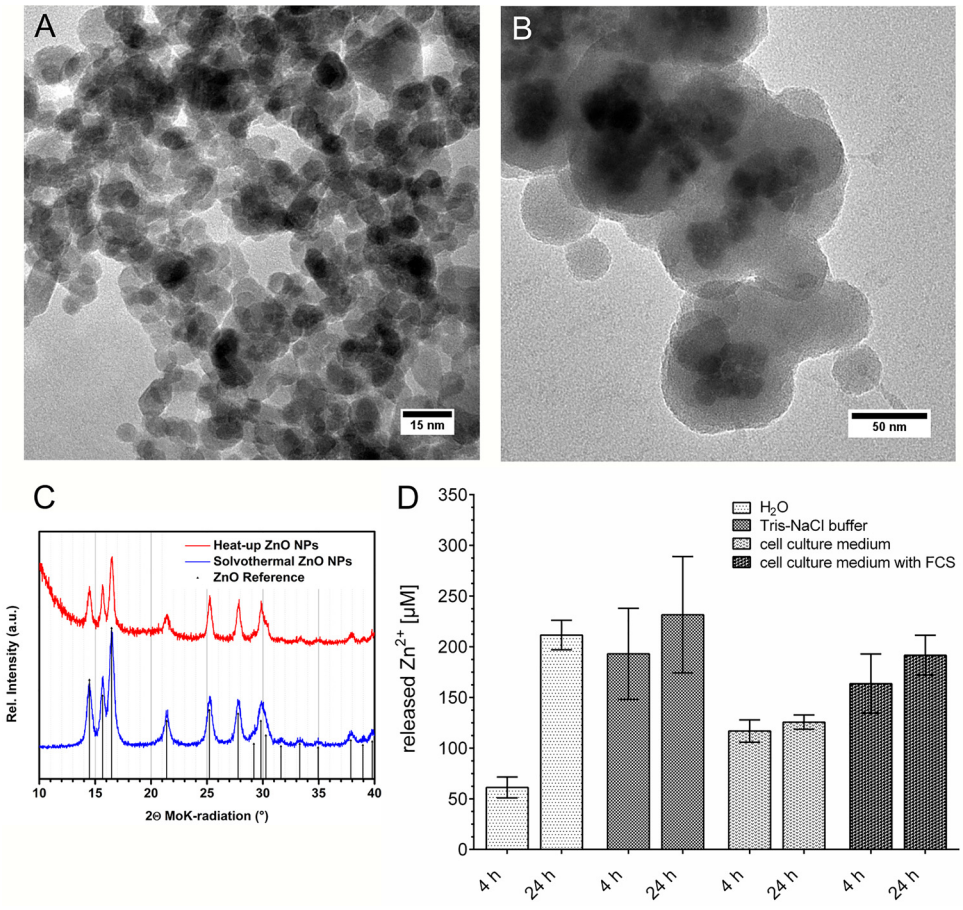


**Fig. 1.** Characterization of ZnO NP and ZnO@$SiO_2$ NP.
TEM imaging (A, B) showed spherical ZnO nanoparticles, 5–15 nm in size. ZnO@$SiO_2$ NP were coated with a silica shell (B) of about 21 nm thickness. The wurtzite-type crystal structure of the ZnO could be verified by X-ray diffraction measurements (C). The release rate of zinc ions by ZnO NP was determined in different buffers (D): at most one fourth of all zinc ions are released within 24 h. Dissolution equilibrium was already nearly established after 4 h in cell culture medium in contrast to water. The release of zinc ions was higher in cell culture medium with FCS compared to cell culture medium without FCS. Shown are means ± SD, N = 3.

culture medium without zinc ions or ZnO NP. After the treatment (4-7 h and 21-24 h) cells treated with the supernatant were able to recover while cells treated with the particles exhibited further reduced cellular viability.

### 3.3. Zinc overload and particle internalization

To trace zinc internalisation into the tumor cells, cells were preincubated with FluoZin™-3-AM and then treated with ZnO NP. We could observe a fast increase in intracellular zinc concentration already within the first 10 min after beginning of the treatment. Fig. 5A shows representative images of HNSCCUM-02 T cells treated with ZnO NP. In green one can see the FluoZin™-3-AM fluorescence indicating the intracellular zinc concentration.

Additionally, to the massive increase in cellular zinc concentration we were also able to show some overlap between zinc-containing

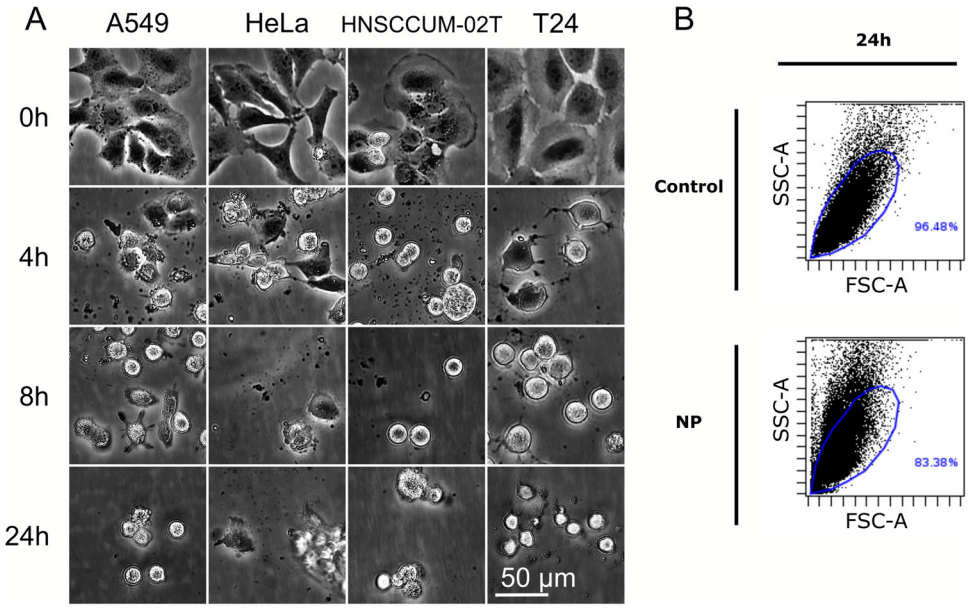


**Fig. 2.** Cellular morphology after ZnO NP treatment.
A549, HeLa, HNSCCUM-02T and T24 cells were treated with 100 µg/mL ZnO NP for 4 h and imaged by light microscopy before the treatment (0 h) and 4 h, 8 h, and 24 h after beginning of the treatment. All tumor cell lines showed pronounced cell rounding followed by detachment from the cell culture plate (A). This was accompanied by a decrease in cell size and increase in granularity compared to untreated control cells, which could be verified by FACS analysis of A549 24 h after beginning of the treatment (B). Representative images of at least N = 3 experiments are shown.

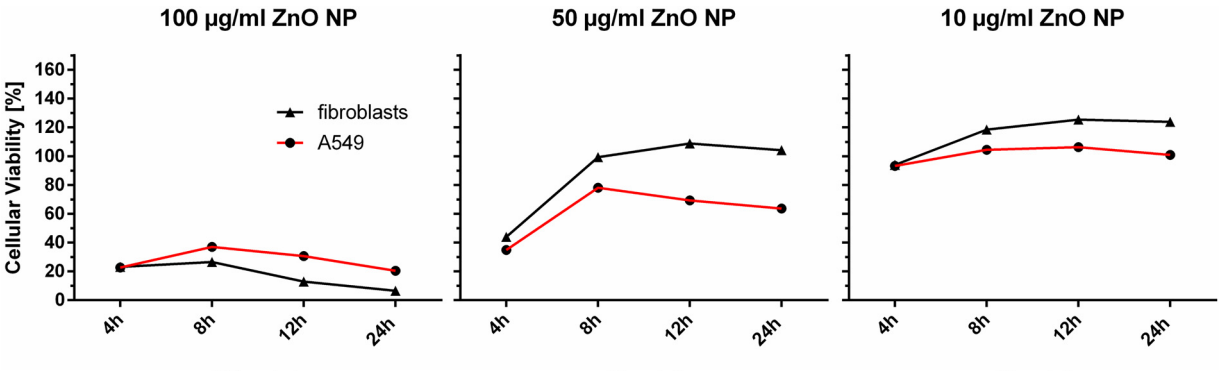


100 µg/ml

| | A549 tumor cells | | | fibroblasts | | |
|---|---|---|---|---|---|---|
| | Mean | SD | N | Mean | SD | N |
| 4h | 23 | 9 | 4 | 23 | 7 | 4 |
| 8h | 37 | 13 | 4 | 27 | 25 | 4 |
| 12h | 31 | 15 | 4 | 13 | 21 | 4 |
| 24h | 21 | 13 | 4 | 7 | 11 | 4 |

50 µg/ml

| | A549 tumor cells | | | fibroblasts | | |
|---|---|---|---|---|---|---|
| | Mean | SD | N | Mean | SD | N |
| 4h | 35 | 12 | 4 | 44 | 15 | 4 |
| 8h | 78 | 9 | 4 | 99 | 25 | 4 |
| 12h | 69 | 21 | 4 | 109 | 42 | 4 |
| 24h | 64 | 24 | 4 | 104 | 47 | 4 |

10 µg/ml

| | A549 tumor cells | | | fibroblasts | | |
|---|---|---|---|---|---|---|
| | Mean | SD | N | Mean | SD | N |
| 4h | 93 | 14 | 4 | 94 | 6 | 4 |
| 8h | 104 | 5 | 4 | 118 | 40 | 4 |
| 12h | 106 | 6 | 4 | 125 | 36 | 4 |
| 24h | 101 | 10 | 4 | 124 | 41 | 4 |

**Fig. 3.** Cytotoxicity of ZnO NP to tumor cells and fibroblasts.
A549 cells and human fibroblasts were subjected to treatment with 100 µg/mL, 50 µg/mL or 10 µg/mL of ZnO NP respectively for 4 h. Their cellular viability was assessed 4 h, 8 h, 12 h and 24 h after beginning of the NP treatment. 100 µg/mL ZnO NP were able to substantially damage both cell types while 10 µg/mL ZnO NP did not do any lasting damage. For 50 µg/mL ZnO NP we could see that tumor cells were damaged while fibroblasts were able to recover from the treatment. Shown in the graph are the means as indicated below. Differences between the experimental groups did not reach statistical significance due to major variation between the biological replicates.

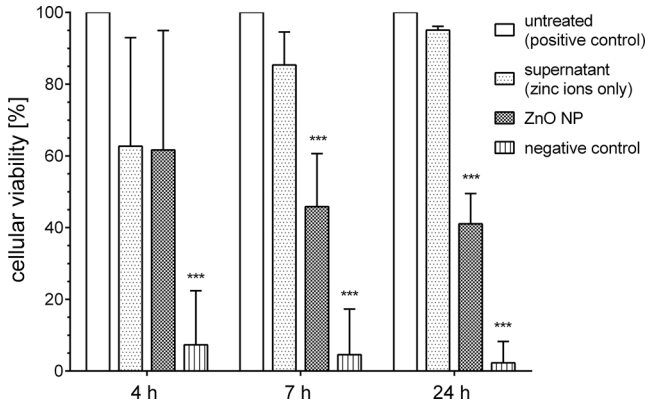


**Fig. 4.** ZnO NP related toxicity is attributable to dissolved zinc ions as well as to direct cell-particle interaction.
Cellular viability of A549 cells was reduced to 60% compared to untreated control cells within 4 h of treatment with 100 µg/mL ZnO NP or supernatant of particles (zinc ions only), respectively. Then cells were washed, and cell culture medium was replaced by fresh medium without NP or zinc ions. Cells which were treated initially with particles showed decreasing viability within 24 h after treatment. On the contrary those cells which were incubated with zinc ions only were able to recover from the treatment by 24 h after beginning of the treatment. Cellular viability was assessed via alamar-Blue® assay. Shown are means ± SD, * $p < 0.05$, ** $p < 0.01$, *** $p < 0.001$, one-way ANOVA, comparison between experimental groups and untreated control, correction for multiple comparisons by Bonferroni, N = 3.

vesicles and lysosomes via simultaneous staining with LysoTracker® Deep Red 60 min after beginning of the ZnO NP treatment (Fig. 5B). A merged picture of the FluoZin™-3-AM channel and the LysoTracker® Deep Red channel are shown in the third column of Fig. 5B, were co-localization of both dyes is shown in yellow in the cLSM image.

To track ZnO NP we designed ZnO@$SiO_2$ NP that are covered by a silica coating which contains FITC. With the help of confocal laser scanning microscopy, we were able to show that those particles were indeed internalized by different tumor cell lines within 4 h (Fig. 5C, I: A549; II: HNSCCUM-02 T; III: FaDu; IV: RPMI-2650). Many particles were attached to the outer cellular membrane stained by CellMask™ Orange Plasma membrane stain and others were already internalized, which could be verified by taking pictures along a z-stack at different focal planes.

### 3.4. Zinc oxide nanoparticles covered by a silica shell evoke delayed cytotoxicity

Comparison of the cytotoxicity of ZnO NP and those covered with a silica shell shows that both types of nanoparticles induce approximately the same toxicity after 24 h but compared to ZnO NP the onset of the cytotoxicity of the ZnO@$SiO_2$ NP is delayed (Fig. 6). After 4 h incubation ZnO NP were able to significantly decrease cellular viability but ZnO@$SiO_2$ NP were not. After 6 h the toxicity of ZnO@$SiO_2$ NP started. After 24 h both types of nanoparticles showed approximately the same extent of toxicity.

### 3.5. Zinc oxide nanoparticles induce apoptotic cell death

Since we could see pronounced cellular toxicity induced by the ZnO NP we finally posed the question, whether apoptosis is induced or whether unspecific toxicity resulted in necrotic processes leading to cell death. We performed a flow cytometric assay using propidium iodide as a marker for the intactness of the outer cellular membrane and Annexin-FITC as apoptotic marker. Fig. 7A shows a representative panel of stained cells treated with ZnO NP for 4 h, analyzed after 4 h, 12 h, 18 h, 24 h, and 48 h after the beginning of the treatment. The intact, living cells are in the lower left quadrant, the (early) apoptotic cells are located in the upper left quadrant, dead cells (either late apoptotic or necrotic) lie in the upper right quadrant and necrotic cells in the lower right quadrant.

The number of dead cells and apoptotic cells rapidly increased after ZnO NP treatment while the population of healthy/intact cells decreased. After 48 h the number of living cells was significantly decreased after treatment with 100 µg/mL ZnO NP or 100 µg/mL $ZnCl_2$ compared to control cells and the number of apoptotic and dead cells in both samples was significantly increased (Fig. 7B). The relative number of necrotic cells in all samples was small. $ZnCl_2$ is completely dissolved in aqueous media, thus it is a suitable control to assess the effect of the released zinc ions, neglecting the effect of the particles themselves. If

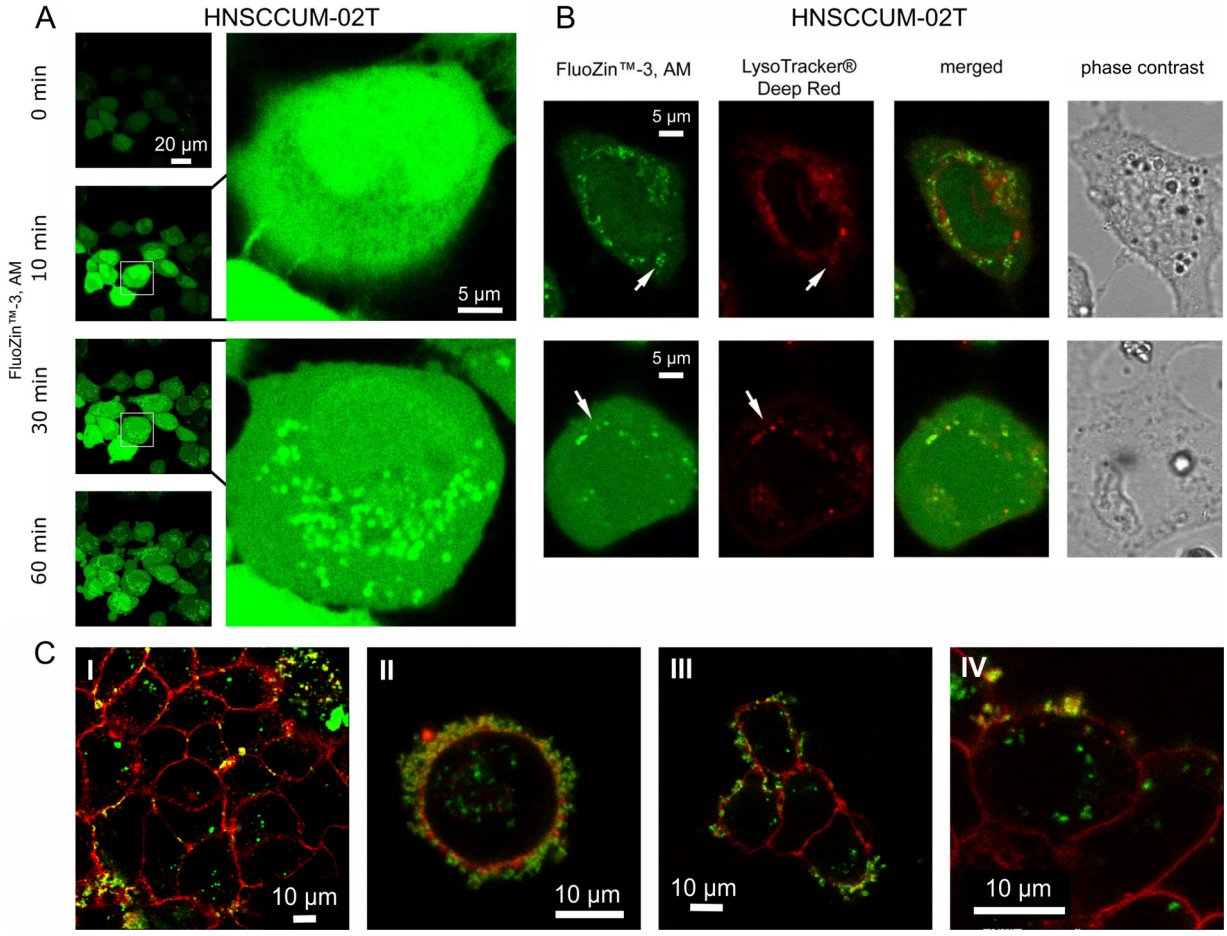


**Fig. 5.** Massive influx of zinc ions after ZnO NP treatment and uptake of $ZnO@SiO_2$ NP.
Confocal laser scanning microscopy with the zinc specific FluoZin™-3AM dye showed a massive influx of zinc ions (green = $Zn^{2+}$) after the treatment of HNSCCUM02 T cells with 100 µg/mL ZnO NP within 10–60 min (A). Additionally, it could be seen that some of the zinc containing vesicles that could be detected 60 min after the treatment, colocalized with lysosomes (B). $ZnO@SiO_2$ NP were taken up by A549 (C I), HNSCCUM-02 T (C II), FaDu (C III) and RPMI-2650 (C IV) cells within 4 h. Furthermore, additional particles could be seen on the cellular surface. Green indicates the position of the NP containing FITC in the silica shell and red the cellular membrane (C). Representative images of N = 3 (A, B) and N = 1 (C) experiments are shown.

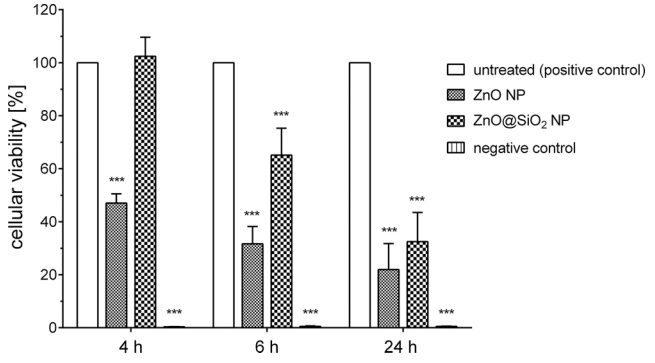


**Fig. 6.** $ZnO@SiO_2$ NP induce delayed cytotoxicity compared to ZnO NP.
A549 cells were subjected to 100 µg/mL ZnO NP or an equivalent amount of $ZnO@SiO_2$ NP, respectively, for the indicated the time points. ZnO NP and $ZnO@SiO_2$ induced approximately the same toxicity within 24 h but compared to ZnO NP the onset of the cytotoxicity of the $ZnO@SiO_2$ was delayed. After 4 h there was a significant decrease in cellular viability after incubation with ZnO NP but not with $ZnO@SiO_2$. After 6 h of incubation with $ZnO@SiO_2$ cellular viability began to decrease. Shown are means ± SD, * $p < 0.05$, ** $p < 0.01$, *** $p < 0.001$, one-way ANOVA, comparison between experimental groups and untreated control, correction for multiple comparisons by Bonferroni, N = 3.

we consider that the amount of zinc ions that was set free by 100 µg/mL ZnO NP within the incubation time did not exceed 300 µM, 40 µg/mL $ZnCl_2$ roughly represents this amount of zinc ions. Thus, treatment of tumor cells with 40 µg/mL $ZnCl_2$ represents an upper border for the effect of the ZnO NP if only extracellularly released zinc ions were relevant. The flow cytometric assay showed that 40 µg/mL $ZnCl_2$ was not able to induce pronounced cell death, the number of living cells was only slightly reduced after 48 h and the number of apoptotic cells was enhanced only to minor extent.

## 4. Discussion

Zinc oxide nanoparticles are considered to have very promising characteristics as an innovative antitumor agent [30]. However, the mechanism of cytotoxicity of ZnO NP is still subject to discussions. To improve the understanding of the cellular processes following exposure to ZnO NP, we wanted to shed light on three main questions:

- Is the cytotoxicity exclusively attributable to extracellularly released zinc ions or also to direct interaction between ZnO NP and cells?
- Are the nanoparticles taken up into tumor cells?
- Which type of cell death is induced by the ZnO NP, necrosis or apoptosis?

For our analyses we chose two different zinc oxide nanoparticles, on

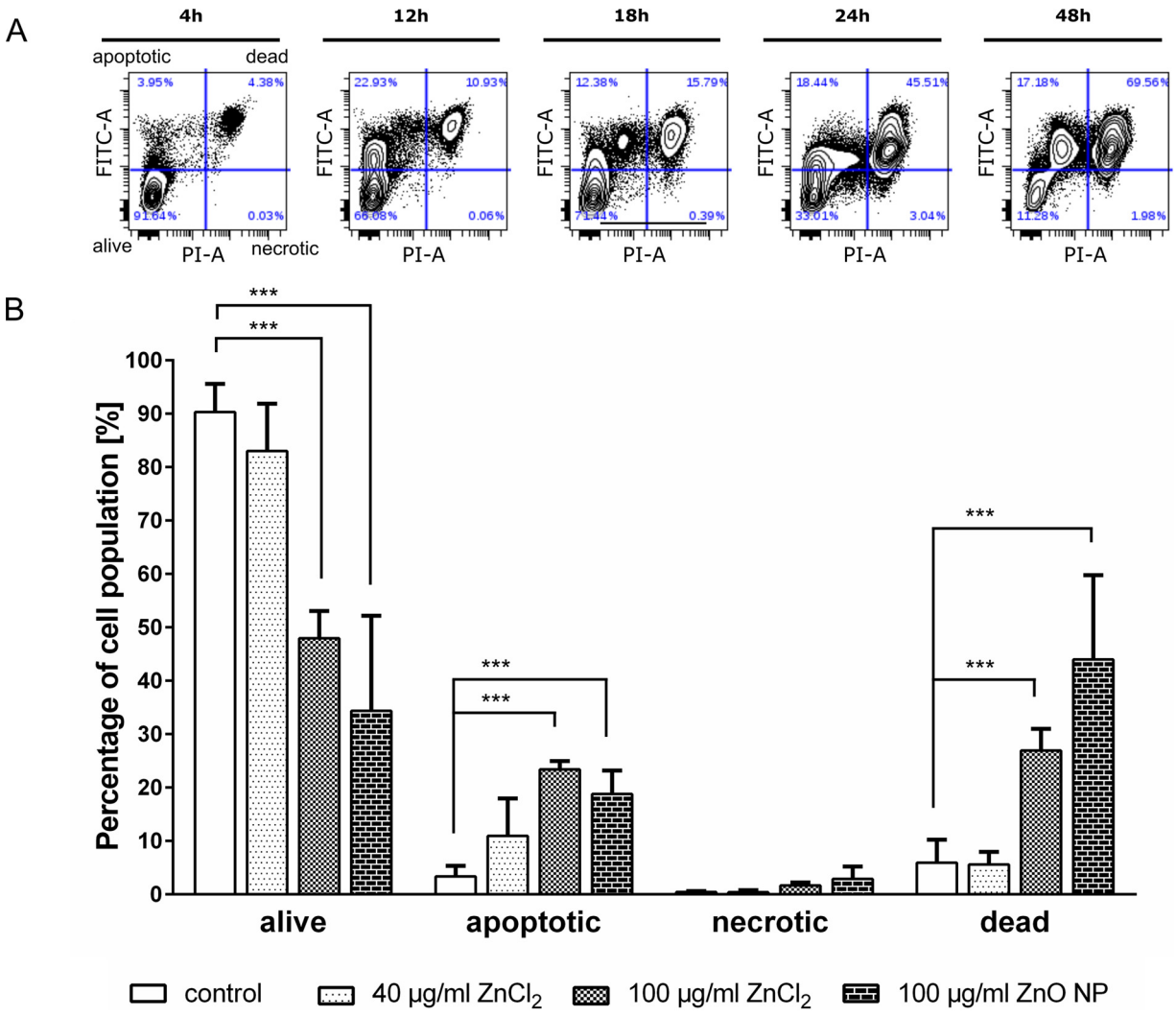


**Fig. 7.** ZnO NP treatment induces cell death via apoptosis.
The type of tumor cell death was explored via staining with propidium iodide (PI) and annexinV-FITC and subsequent flow cytometric analysis. In Fig. 7A a representative compilation of staining results of A549 cells treated with 100 µg/mL ZnO NP can be seen 4 h, 12 h, 18 h, 24 h, and 48 h after beginning of the treatment. In the lower left quadrant living cells are located, in the upper left quadrant apoptotic cells can be seen, in the upper right quadrant dead cells and in the lower right quadrant necrotic cells. The cell population migrated first upwards over time and then to the right indicating the induction of apoptosis and subsequent cell death. 48 h after beginning of the treatment (B) the number of living cells was significantly decreased and the number of apoptotic and dead cells was significantly increased in those cell populations which were treated with 100 µg/mL ZnO NP or 100 µg/mL $ZnCl_2$ respectively. 40 µg/mL $ZnCl_2$ was not able to induce significant cell death. Shown are means ± SD, * $p < 0.05$, ** $p < 0.01$, *** $p < 0.001$, two-way ANOVA, comparison between experimental groups and untreated control, correction for multiple comparisons by Bonferroni, N = 6.

the one hand "naked" ZnO NP which did not receive any surface treatment and on the other hand ZnO@$SiO_2$ NP which were covered with a silica shell in which the fluorescent dye FITC was incorporated to be able to track them by fluorescent microscopy.

One repeatedly emerging controversial issue is the question whether the effect of ZnO NP on tumor cells is exerted by zinc ions that are rapidly liberated from the NP outside the cells. To address this question, we first quantified the amount of zinc ions that was released from the particles within 4 h and 24 h in several buffers. The time point 4 h was chosen according to our incubation time with the NP in the following experiments. The dissolution equilibrium in cell culture medium was already nearly established after 4 h and the amount of additional zinc ions that was set free within the subsequent 20 h was low. In total 100 µg/mL ZnO NP could theoretically set free 1,23 mM zinc ions but only at most 250 to 300 µM zinc ions were released, one fourth of the amount that could be possible. This clearly shows that the particles are not completely disintegrated extracellularly. The amount of released zinc ions was higher in cell culture media with FCS than in cell culture medium without. This effect could result from the higher number of biomolecules in the media with FCS, which could bind zinc ions and thus remove them from the equilibrium, so that additional zinc ions are released. All in all, we can conclude that there is the possibility that the ZnO NP directly interact with the cells, not only taking effects via released zinc ions, as the particles do not disintegrate completely and only at most 25% of the zinc ions are released from the NP.

To test whether the observed cell toxicity can be traced back to the particles or to released zinc ions we compared the effect of ions and particles in a viability assay. Both zinc ions and ZnO NP reduced the cellular viability within 4 h to the same extend. Then the cells were washed, and the cell culture medium containing zinc ions or ZnO NP respectively was replaced by fresh medium. The cells that have been treated with zinc ions alone recovered within 24 h from the treatment. On the contrary, cells which were treated with NP, exhibited significantly reduced cellular viability after 24 h. This finally proves that the cytotoxicity of ZnO NP cannot be traced back exclusively to the release of zinc ions outside the cells. It must be considered that the

particles directly interact with the tumor cells.

To further investigate this issue, we performed confocal laser scanning microscopy. This revealed that treatment with ZnO NP is associated with a fast influx of zinc ions. Some of the vesicular structures that contained zinc, were found to co-localize with lysosomes. This suggests that the endolysosomal compartment is involved in the uptake of zinc even though other routes of entry must be considered concerning the fact that only a small amount of zinc co-localized with the lysosomes. Additionally, we could prove that ZnO@$SiO_2$ NP directly interact with the tumors cells in two ways: ZnO@$SiO_2$ NP are deposited in huge amounts on the cellular membrane and they are internalized by tumor cells. This supports that cellular toxicity of ZnO NP is not only attributable to liberated zinc ions but also to a direct interaction between the nanomaterial and the tumor cells.

We directly compared the cellular toxicity of ZnO NP and ZnO@$SiO_2$ NP and we found that both types of nanoparticles induce approximately the same reduction in cellular viability after 24 h but the toxicity of ZnO@$SiO_2$ NP was delayed compared to the pristine particles. This is a desirable effect in a future perspective as it could enable to safely transport the particles through the blood stream to the tumor site. Moreover, this shows that the ZnO@$SiO_2$ NP that stick to the cellular surface and those which are taken up after 4 h incubation can approximately have the same but time-delayed effect on the cellular viability as pristine ZnO NP which induce a fast increase in intracellular zinc concentrations. This suggests that ZnO@$SiO_2$ NP time-dependently liberate zinc ions within the cell, which in the end also leads to a fatal increase in intracellular zinc ion concentrations. Possibly, zinc oxide nanoparticles can also directly damage the cellular membrane and cytoskeletal defects as well as loss of intracellular interactions and adhesive properties were already described [25,31–33]. However, as ZnO NP and ZnO@$SiO_2$ NP could induce similar toxicity after 24 h our data supports the assumption that the nanoparticles take effect via internalisation and increase of intracellular zinc ion concentration.

Those NP that were internalized could induce toxicity via different mechanisms. NP are characterized by a high surface to volume ratio, which is typically associated with an increased surface reactivity [34]. This is additionally fostered by lattice defects at the surface of ZnO NP [35]. Reactive oxygen species (ROS) can be generated directly on the nanoparticle surface and particles could also get further dissolved intracellularly [36]. Zinc ions liberated within the cell could disrupt the intracellular ion homeostasis and damage cellular organelles such as mitochondria [37] or biomolecules such as proteins and DNA [38].

Concerning the cytotoxicity of ZnO NP towards human tumour cells in comparison to “normal” fibroblasts as representatives of healthy tissue we assessed cell viability after treatment with 100 µg/mL, 50 µg/mL and 10 µg/mL ZnO NP. While a dosage of 100 µg/mL ZnO NP was able to damage healthy and tumorous cell lines, 10 µg/mL ZnO NP were not able to do substantial damage to the cells. For the intermediate concentration of 50 µg/mL we could see a selective toxicity towards the tumor cells while fibroblasts were able to recover from the treatment. This shows that preferential tumor cell death could in theory be possible, especially if we consider a local concentration of the NP at the tumor site via passive or active targeting. Additionally, it should be considered that the fibroblasts used in this experiment are primary cells which are more sensitive to manipulations than an established tumor cell line, which could have experienced certain changes during cultivation which distinguishes it from the original primary tumor cells.

Since we observed cellular toxicity, we wanted to elucidate whether the tumor cells die via apoptotic or via necrotic cell death. Regarding the cellular morphology after ZnO NP treatment it could be observed that all tested tumor cell lines showed a pronounced cell rounding, followed by detachment from the cell culture plate. This was accompanied by a decrease in size and an increase in granularity, both being typical features of apoptotic cell death [39]. With a flow cytometric assay, we assessed the proportions of living, apoptotic, necrotic and dead cells in the cell population after treatment with ZnO NP. The percentage of apoptotic and dead cells significantly increased within 48 h after the treatment with ZnO NP while the percentage of living cells decreased to 3050% compared to untreated control cells. Treatment of tumor cells with 100 µg/mL $ZnCl_2$ also significantly reduced cell viability, though the effect was not that pronounced as after treatment with ZnO NP. This clearly shows that an overload with zinc ions can induce apoptotic cell death in tumor cells. The percentage of necrotic cells was low and did not significantly increase after ZnO NP treatment, thus necrosis can be regarded to be less frequent. These findings are supported by the morphological changes we observed after ZnO NP treatment which also suggest apoptotic cell death. 40 µg/mL $ZnCl_2$ roughly represent the amount of zinc ions that is set free by 100 µg/mL ZnO NP, thus it can serve as a control to estimate the sole effect of the zinc ions that are released from the NP. It could be seen, that 40 µg/mL $ZnCl_2$ were not able to significantly reduce the proportion of living cells. Thus, the flow cytometric assay confirms that the cytotoxicity of ZnO NP could not be attributed to zinc ions only, that are released extracellularly from the ZnO NP.

In summary, our experiments show that ZnO NP can exert cytotoxic effects on tumor cells, which are attributable to the release of zinc ions outside the cells as well as to a direct interaction between NP and cells. Tumor cell damage finally cumulates in apoptotic cell death, which is induced by a massive influx of zinc ions, as well as by nanoparticle-cell interaction and nanoparticle uptake. A therapeutical perspective could be the targeted accumulation of ZnO NP at the tumor side to induce zinc overload that substantially damages the tumor cells. This should result in tumor cell death, while healthy tissue remains largely unaffected. The residual ZnO NP could be easily cleared by the body. Low zinc concentrations as well as bulk zinc oxide are recognized as a Generally Regarded as Safe (GRAS) substance by the US Food and Drug Administration (FDA) [40]. Altogether this study shows that ZnO NP have promising characteristics for an application as innovative antitumor agent.

## Funding

This work was supported by the Max Planck Graduate Center with the Johannes Gutenberg-Universität Mainz (MPGC) and the focus program BiomaTiCS of the University Medical Center, Mainz.

## Conflicts of interest statement

None declared.

## Acknowledgments

We thank Simone Mendler, Karin Benz and Rita Gieringer for their excellent technical assistance and the Max Planck Graduate Center with the Johannes Gutenberg-Universität Mainz (MPGC) and the focus group Biomaterials, Tissues and Cells in Science (BiomatTiCS) for financial support. We also thank Anke Kaltbeitzel and Jonas Reinholz of the Max Planck Institute for Polymer Research (MPIP) for the excellent technical support at the cLSM.

## References

[1] H. Goesmann, C. Feldmann, Nanoparticulate functional materials, Angew. Chem. (Int. Ed.) 49 (8) (2010) 1362–1395.
[2] C. Bai, M. Liu, From chemistry to nanoscience: not just a matter of size, Angew. Chem. (Int. Ed.) 52 (2013) 2678–2683.
[3] T.D. Schladt, K. Schneider, H. Schild, W. Tremel, Synthesis and bio-functionalization of magnetic nanoparticles for medical diagnosis and treatment, J. Chem. Soc. Dalton Trans. 40 (24) (2011) 6315–6343.
[4] J.W. Rasmussen, E. Martinez, P. Louka, D.G. Wingett, Zinc oxide nanoparticles for selective destruction of tumor cells and potential for drug delivery applications, Expert Opin. Drug Deliv. 7 (9) (2010) 1063–1077.
[5] A.E. Nel, L. Madler, D. Velegol, T. Xia, E.M.V. Hoek, P. Somasundaran, F. Klaessig, V. Castranova, M. Thompson, Understanding biophysicochemical interactions at

the nano-bio interface, Nat. Mater. 8 (7) (2009) 543–557.
[6] T. Sun, Y.S. Zhang, B. Pang, D.C. Hyun, M. Yang, Y. Xia, Engineered nanoparticles for drug delivery in cancer therapy, Angew. Chem. (Int. Ed.) 53 (46) (2014) 12320–12364.
[7] P. Singh, A. Nanda, Enhanced sun protection of nano-sized metal oxide particles over conventional metal oxide particles: an in vitro comparative study, Int. J. Cosmet. Sci. 36 (3) (2014) 273–283.
[8] A. Kołodziejczak-Radzimska, T. Jesionowski, Zinc oxide-from synthesis to application: a review, Materials 7 (4) (2014) 2833–2881.
[9] A. Sirelkhatim, S. Mahmud, A. Seeni, N.H.M. Kaus, L.C. Ann, S.K.M. Bakhori, H. Hasan, D. Mohamad, Review on zinc oxide nanoparticles: antibacterial activity and toxicity mechanism, Nano-micro Lett. 7 (3) (2015) 219–242.
[10] C. Hanley, J. Layne, A. Punnoose, K.M. Reddy, I. Coombs, A. Coombs, K. Feris, D. Wingett, Preferential killing of cancer cells and activated human T cells using ZnO nanoparticles, Nanotechnology 19 (29) (2008) 295103.
[11] R.J. Vandebriel, W.H. de Jong, A review of mammalian toxicity of ZnO nanoparticles, Nanotechnol. Sci. Appl. 5 (2012) 61–71.
[12] M. Pandurangan, G. Enkhtaivan, D.H. Kim, Anticancer studies of synthesized ZnO nanoparticles against human cervical carcinoma cells, J. Photochem. Photobiol. B Biol. 158 (2016) 206–211.
[13] R. Wahab, N. Kaushik, F. Khan, N.K. Kaushik, E.H. Choi, J. Musarrat, A.A. Al-Khedhairy, Self-styled ZnO nanostructures promotes the Cancer cell damage and supresses the epithelial phenotype of glioblastoma, Sci. Rep. 6 (2016) 19950.
[14] R. Wahab, M.A. Siddiqui, Q. Saquib, S. Dwivedi, J. Ahmad, J. Musarrat, A.A. Al-Khedhairy, H.-S. Shin, ZnO nanoparticles induced oxidative stress and apoptosis in HepG2 and MCF-7 cancer cells and their antibacterial activity, Colloids Surf. B Biointerfaces 117 (2014) 267–276.
[15] M. Chandrasekaran, M. Pandurangan, In vitro selective anti-proliferative effect of zinc oxide nanoparticles against Co-cultured C2C12 myoblastoma Cancer and 3T3-L1 normal cells, Biol. Trace Elem. Res. (2015) 148–154.
[16] M. Premanathan, K. Karthikeyan, K. Jeyasubramanian, G. Manivannan, Selective toxicity of ZnO nanoparticles toward Gram-positive bacteria and cancer cells by apoptosis through lipid peroxidation, Nanomed. Nanotechnol. Biol. Med. 7 (2) (2011) 184–192.
[17] J. Gupta, P. Bhargava, D. Bahadur, Fluorescent ZnO for imaging and induction of DNA fragmentation and ROS-mediated apoptosis in cancer cells, J. Mater. Chem. B 3 (9) (2015) 1968–1978.
[18] S. Ostrovsky, G. Kazimirsky, A. Gedanken, C. Brodie, Selective cytotoxic effect of ZnO nanoparticles on glioma cells, Nano Res. 2 (11) (2009) 882–890.
[19] K.C. Biplab, S.N. Paudel, S. Rayamajhi, D. Karna, S. Adhikari, B.G. Shrestha, G. Bisht, Enhanced preferential cytotoxicity through surface modification: synthesis, characterization and comparative in vitro evaluation of TritonX-100 modified and unmodified zinc oxide nanoparticles in human breast cancer cell (MDA-MB-231), Chem. Cent. J. 10 (1) (2016) 1063.
[20] L. Taccola, V. Raffa, C. Riggio, O. Vittorio, M.C. Iorio, R. Vanacore, A. Pietrabissa, A. Cuschieri, Zinc oxide nanoparticles as selective killers of proliferating cells, Int. J. Nanomedicine 6 (2011) 1129–1140.
[21] A. Sasidharan, P. Chandran, D. Menon, S. Raman, S. Nair, M. Koyakutty, Rapid dissolution of ZnO nanocrystals in acidic cancer microenvironment leading to preferential apoptosis, Nanoscale 3 (9) (2011) 3657–3669.
[22] M.J. Akhtar, M. Ahamed, S. Kumar, M.M. Khan, J. Ahmad, S.A. Alrokayan, Zinc oxide nanoparticles selectively induce apoptosis in human cancer cells through reactive oxygen species, Int. J. Nanomedicine 7 (2012) 845–857.
[23] S. Alarifi, D. Ali, S. Alkahtani, A. Verma, M. Ahamed, M. Ahmed, H.A. Alhadlaq, Induction of oxidative stress, DNA damage, and apoptosis in a malignant human skin melanoma cell line after exposure to zinc oxide nanoparticles, Int. J. Nanomedicine 8 (2013) 983–993.
[24] H.F.H. Hassan, A.M. Mansour, A.M.H. Abo-Youssef, B.E.M. Elsadek, B.A.S. Messiha, Zinc oxide nanoparticles as a novel anticancer approach; in vitro and in vivo evidence, Clin. Exp. Pharmacol. Physiol. 44 (2) (2017) 235–243.
[25] S.R. Choudhury, J. Ordaz, C.-L. Lo, N.P. Damayanti, F. Zhou, J. Irudayaraj, Zinc oxide nanoparticles-induced reactive oxygen species promotes multimodal cyto- and epigenetic toxicity, Toxicol. Sci. 156 (1) (2017) 261–274.
[26] B. Cheng, W. Shi, J.M. Russell-Tanner, L. Zhang, E.T. Samulski, Synthesis of variable-aspect-ratio, single-crystalline ZnO nanostructures, Inorg. Chem. 45 (3) (2006) 1208–1214.
[27] M.N. Tahir, F. Natalio, M.A. Cambaz, M. Panthöfer, R. Branscheid, U. Kolb, W. Tremel, Controlled synthesis of linear and branched Au@ZnO hybrid nanocrystals and their photocatalytic properties, Nanoscale 5 (20) (2013) 9944–9949.
[28] H.-J. Welkoborsky, R. Jacob, S.H. Riazimand, H.S. Bernauer, W.J. Mann, Molecular biologic characteristics of seven new cell lines of squamous cell carcinomas of the head and neck and comparison to fresh tumor tissue, Oncology 65 (1) (2003) 60–71.
[29] M. Heller, E.V. Frerick-Ochs, H.-K. Bauer, E. Schiegnitz, D. Flesch, J. Brieger, R. Stein, B. Al-Nawas, C. Brochhausen, J.W. Thüroff, R.E. Unger, W. Brenner, Tissue engineered pre-vascularized buccal mucosa equivalents utilizing a primary triculture of epithelial cells, endothelial cells and fibroblasts, Biomaterials 77 (2016) 207–215.
[30] P.K. Mishra, H. Mishra, A. Ekielski, S. Talegaonkar, B. Vaidya, Zinc oxide nanoparticles: a promising nanomaterial for biomedical applications, Drug Discov. Today 22 (12) (2017) 1825–1834.
[31] R. Pati, I. Das, R.K. Mehta, R. Sahu, A. Sonawane, Zinc-oxide nanoparticles exhibit genotoxic, Clastogenic, cytotoxic and actin depolymerization effects by inducing oxidative stress responses in macrophages and adult mice, Toxicol. Sci. 150 (2) (2016) 454–472.
[32] E. Paszek, J. Czyz, O. Woźnicka, D. Jakubiak, J. Wojnarowicz, W. Łojkowski, E. Stępień, Zinc oxide nanoparticles impair the integrity of human umbilical vein endothelial cell monolayer in vitro, J. Biomed. Nanotechnol. 8 (6) (2012) 957–967.
[33] L. Garcia-Hevia, R. Valiente, R. Martin-Rodriguez, C. Renero-Lecuna, J. Gonzalez, L. Rodriguez-Fernandez, F. Aguado, J.C. Villegas, M.L. Fanarraga, Nano-ZnO leads to tubulin macrotube assembly and actin bundling, triggering cytoskeletal catastrophe and cell necrosis, Nanoscale 8 (21) (2016) 10963–10973.
[34] V.H. Grassian, When Size Really Matters: Size-Dependent Properties and Surface Chemistry of Metal and Metal Oxide Nanoparticles in Gas and Liquid Phase Environments, J. Phys. Chem. C 112 (47) (2008) 18303–18313.
[35] V. Lakshmi Prasanna, R. Vijayaraghavan, Insight into the mechanism of antibacterial activity of ZnO: surface defects mediated reactive oxygen species even in the dark, Langmuir 31 (33) (2015) 9155–9162.
[36] C. Shen, S.A. James, M.D. de Jonge, T.W. Turney, P.F.A. Wright, B.N. Feltis, Relating cytotoxicity, zinc ions, and reactive oxygen in ZnO nanoparticle-exposed human immune cells, Toxicol. Sci. 136 (1) (2013) 120–130.
[37] Y.-Y. Kao, Y.-C. Chen, T.-J. Cheng, Y.-M. Chiung, P.-S. Liu, Zinc oxide nanoparticles interfere with zinc ion homeostasis to cause cytotoxicity, Toxicol. Sci. 125 (2) (2012) 462–472.
[38] M. Condello, B. de Berardis, M.G. Ammendolia, F. Barone, G. Condello, P. Degan, S. Meschini, ZnO nanoparticle tracking from uptake to genotoxic damage in human colon carcinoma cells, Toxicol. Vitro 35 (2016) 169–179.
[39] Susan Elmore, Apoptosis: a review of programmed cell death, Toxicol. Pathol. 35 (4) (2007) 495–516.
[40] H. Sharma, P.K. Mishra, S. Talegaonkar, B. Vaidya, Metal nanoparticles: a theranostic nanotool against cancer, Drug Discov. Today 20 (9) (2015) 1143–1151.